

# Conditional GLMMs for reaction times in choice tasks

Mauricio Tejo<sup>a,\*</sup>, Cristian Meza<sup>b</sup>, and Fernando Marmolejo-Ramos<sup>c</sup>

<sup>a</sup>*Instituto de Estadística, Universidad de Valparaíso, Chile.*

<sup>b</sup>*Instituto de Ingeniería Matemática, Universidad de Valparaíso, Chile.*

<sup>c</sup>*College of Education, Psychology, and Social Work, Flinders University, Australia.*

*\*Corresponding author: mauricio.tejo@uv.cl*

## Abstract

This study connects two methods for modeling reaction times (RTs) in choice tasks: (1) the first-hitting time of a simple diffusion model with a single barrier, representing the cognitive process leading to a response, and (2) Generalized Linear Mixed Models (GLMMs). We achieve this by analyzing RT distributions conditioned on each response alternative. Because certain diffusion model variants yield Inverse Gaussian (IG) and Gamma distributions for first-hitting times, we can justify using these distributions in RT models. Conversely, employing IG and Gamma distributions within GLMMs allows us to infer the underlying cognitive processes. We demonstrate this concept through simulations and apply it to previously published real-world data. Finally, we discuss the scope and potential extensions of our approach.

**Keywords:** cognitive process; choice task tests; Generalized Linear Mixed Models; Inverse Gaussian distribution; Gamma distribution

# 1 Introduction

## 1.1 Background

In experimental psychology, reaction times (RTs)—the time between a stimulus and a behavioral response—have long been a central focus of study, aiming to understand the processes underlying their distribution [e.g., [Woodrow \(1911\)](#), [Smith \(1968\)](#), [Wainer \(1977\)](#), [Ratcliff \(1978\)](#), [Meyer et al. \(1988\)](#), [Posner \(2005\)](#), [Matzke and Wagenmakers \(2009\)](#), [Baayen and Milin \(2010\)](#), [Balota and Yap \(2011\)](#), [Woods et al. \(2015\)](#), [Donkin and Brown \(2018\)](#), [De Boeck and Jeon \(2019\)](#), [Tejo et al. \(2019\)](#), [Rousselet and Wilcox \(2020\)](#)]. RT models can be broadly classified (not mutually exclusively) as: (1) quantitative distribution measurements, focused on capturing key features of empirical RT distributions; and/or (2) theoretical models, deriving probability distributions based on cognitive mechanisms [e.g., [Matzke and Wagenmakers \(2009\)](#), [Ratcliff and Van Donigen \(2011\)](#), [Anders et al. \(2016\)](#), [Tejo et al. \(2019\)](#)].

A common example of a quantitative RT distribution model is the Ex-Gaussian (EG) distribution, which often provides a good fit to empirical RT data. However, its parameters lack a clear cognitive interpretation [e.g., [Ratcliff \(1978\)](#), [Rohrer and Wixted \(1994\)](#), [Matzke and Wagenmakers \(2009\)](#), [Palmer et al. \(2011\)](#), [Marmolejo-Ramos and González-Burgos \(2013\)](#), [Marmolejo-Ramos, Vélez, and Romão \(2015\)](#), [Marmolejo-Ramos, Cousineau, et al. \(2015\)](#), [Vélez et al. \(2015\)](#), [Osmon et al. \(2018\)](#)]. Conversely, theoretical models aim to derive models based on the cognitive mechanisms underlying responses in choice tests, with model complexity depending on the complexity of the experimental task.

Experimental task complexity varies. In simple-choice (SC) tasks, stimuli are presented one at a time, and participants make one of two possible responses to categorize the stimulus (e.g., a participant views a picture and classifies it as either positive or negative in valence). In multiple-choice (MC) tasks, stimuli are also presented one at a time, but participants must select one of three or more possible responses to categorize the stimulus (e.g., a participant views a picture and classifies it as positive, neutral, or negative in valence). (Here, we assume that individuals are compelled to choose and respond with one of the available options provided in the task.) For SC tasks, theoretical models typically conceptualize the underlying cognitive mechanisms experienced by participants during the task. These models are then used to calculate the first instance at which one of the two response options is emitted.

## 1.2 Preliminaries

Regarding the underlying cognitive mechanism involved in a SC task, a general scheme of a cognitive process, denoted as  $\{X_t\}_{t \in \mathbb{R}_+}$ , may consider a first-time step  $\theta \geq 0$ , during which the individual primarily receives the stimulus and no response can be produced during this time interval. Following this, the decision stage begins by processing the information related to the task's difficulty along with random fluctuations. A response is finally produced when  $X_t$  reaches

one of the two barriers, say 0 or  $b$  (with  $0 < X_\theta < b$ ), for the first time. The distribution of this first-hitting time corresponds to the RT distribution. Depending on the assumed dynamics of  $\{X_t\}_{t \in \mathbb{R}_+}$ , calculating this first-hitting time can be complex [see e.g. [LaBerge \(1962\)](#), [Ratcliff \(1978\)](#), [Ratcliff and Tuerlinckx \(2002\)](#), [Usher et al. \(2002\)](#), [Horrocks and Thompson \(2004\)](#), [Brown and Heathcote \(2008\)](#), [Blurton et al. \(2017\)](#)].

A simplified single-barrier model remains useful as a representation of the cognitive process leading to a specific response. By calculating the RT distribution conditioned on each response alternative, the overall RT distribution can be obtained as a mixture of these conditional distributions, weighted by the marginal probabilities of each response (via the Law of Total Probability, LTP). This principle can be extended to MC tasks.

A simple mathematical representation of the cognitive process in a choice task can be expressed as:

$$X_t = X_\theta - \nu(t - \theta) + e_{t-\theta}, \quad (1)$$

for  $t \geq \theta \in \mathbb{R}_+$ , and  $X_t = X_\theta$  otherwise. Here,  $X_\theta > 0$  represents the initial processing state, with  $\theta$  also known as the “non-decision parameter”;  $\nu$  is the “mean rate of information accumulation” (influenced by individual differences in information processing or stimulus characteristics reflecting task difficulty), and  $\{e_t\}_{t \in \mathbb{R}_+}$  is a stochastic process representing random fluctuations, typically assumed to be a Wiener or Brownian motion process [[Ratcliff and Van Dongen \(2011\)](#), [Tejo et al. \(2019\)](#)]. It is well-known that when  $X_\theta$  and  $\nu$  are assumed to be fixed parameters, such that  $\nu > 0$ , the resulting distribution of the one-barrier first-hitting time after  $\theta$  of  $X_t$  to 0,

$$\tau_0 := \inf\{t > \theta : X_t = 0\}, \quad (2)$$

is a shifted version of the Inverse Gaussian (IG) or Wald distribution. Other distributions within the Gamma and Birnbaum-Saunders (BS) families can be derived for this first-hitting time distribution by modifying assumptions about the components of Equation (1) [[Jackson et al. \(2009\)](#), [Tejo et al. \(2018\)](#), [Tejo et al. \(2019\)](#)]. These resulting distributions serve as simple theoretical RT models that have demonstrated good quantitative fits to real RT data [[Anders et al. \(2016\)](#), [Tejo et al. \(2018\)](#), [Tejo et al. \(2019\)](#)]. However, the specific parameter values will depend on experimental factors, such as the stimuli and their corresponding responses. These experiments require a sufficient number of replications per factor (discussed further later).

Similarly, a connection can be established between the parameters of a set of RTs (e.g., mean and variance) and the parameters of the underlying diffusion process (e.g., starting processing point and mean rate of information accumulation). In other words, given a random sample of RTs and estimating its parameters, we can reconstruct a cognitive scheme like (1) such that  $\tau_0$  (the first hitting time/RT) follows a distribution similar to the original random sample. This is a key focus of this work.

We support the foundation that the validity of a proposed model depends on its performance as a quantitative distribution measurement and its theoretical grounding. Given the varying complexity of choice tasks based on stimuli and responses, a general RT model should incorporate a more complex structure that explicitly considers different stimuli and individual effects as covariates. Generalized Linear Mixed Models (GLMMs) provide such a hierarchical structure [McCulloch and Neuhaus (2005)], linking mean RTs with covariates that specify the relationship between RTs and the applied stimuli. In this framework, the dependent variable is RT, with each stimulus (or stimulus combination) treated as a “fixed effect” at various levels, and “random effects” accounting for individual variability across trials [Tuerlinckx et al. (2006), Lo and Andrews (2015), Stroup (2012), Molenaar et al. (2015), De Boeck and Jeon (2019)]. However, in this work, following the LTP, we will use GLMMs to model the RT distribution conditioned on each alternative response.

Often, responses are classified as correct or incorrect based on their congruence with the presented stimuli [e.g., De Boeck and Jeon (2019)]; in these cases, the two-barrier model represents a choice between a correct and an incorrect response. However, this classification is not always straightforward. For instance, Marmolejo-Ramos et al. (2020) presented participants with a spectrum of facial expressions, from happiest to saddest, asking them to classify each as “happy” or “sad.” “Intermediate” expressions were essentially neutral (neither happy nor sad), making a clear “correct”/“incorrect” classification difficult. This is even more problematic with diverse stimuli like landscapes, where similar categorization is required. Therefore, it is generally more useful to analyze the responses themselves, examining their frequency and dispersion at each stimulus level. When responses can be reliably categorized as “correct” or “incorrect,” a more in-depth analysis can determine which stimulus levels lead to higher error rates.

Candidate models for the RT distribution, conditioned on each possible response, can be justified by the theoretical arguments concerning one-barrier first-hitting time distributions. Some resulting distributions, such as the IG and Gamma, are suitable for GLMMs as they belong to the Exponential Family. The BS distribution, closely related to the IG distribution [Desmond (1986), Balakrishnan et al. (2009), Leiva et al. (2015)], has been recently proposed as a theoretical model for simple-choice RTs [Ranger et al. (2015), Tejo et al. (2018), Tejo et al. (2019)], but is not directly supported within standard GLMMs. While Villegas et al. (2011) developed a constructive linear mixed model similar to GLMMs for the logarithm of the dependent variable, we will not consider the BS distribution here. This is because transforming the RTs distorts their ratio scale properties [Lo and Andrews (2015)], and transforming back to the original RT scale to infer the underlying cognitive process introduces transformations and approximations that could lead to significant errors. Furthermore, deriving BS-distributed stopping times from a diffusion process like (1) is an approximation, unlike the exact derivation for IG-distributed stopping times [see Tejo et al. (2018)].

To obtain the complete RT distribution, we must also consider the distribution of responses. These can be consistently estimated via frequencies based

on stimuli/trials, although a more structured modeling can be developed (we will discuss this later). As previously mentioned, the LTP allows us to obtain the overall RT distribution: if  $Y$  represents the RT random variable for a given experiment, and  $R_1, R_2, \dots, R_L$  are the possible responses, then the cumulative distribution function of  $Y$  is given by

$$F(y) := P(Y \leq y) = \sum_{l=1}^L P(Y \leq y | R_l) P(R_l).$$

Thus, the distribution of  $Y$  is a mixture of conditional distributions, weighted by the probabilities of the corresponding responses.

Building on the preceding discussion, the next section details our modeling approach and presents simulations demonstrating the reconstruction of (1) for IG and Gamma RTs. Section 3 applies our methodology to a previously published experiment, and Section 4 discusses the scope of our proposal and potential extensions.

## 2 Model approach

We begin by defining a hierarchical structure for the dependent variable (RTs) in a choice task where individuals are presented with various types of stimuli at different levels and asked to choose one of several alternatives as quickly as possible. For illustration, consider two response alternatives,  $R_1$  and  $R_2$ , and different types of stimuli (referred to as “fixed effects”) at various levels. Let  $n$  be the total number of combined levels across all stimulus types. Let  $Y_{ijk}$  denote the  $j$ -th RT of the  $k$ -th individual under the  $i$ -th level, where  $j = 1, \dots, n_i$ ,  $k = 1, \dots, m$  and  $i = 1, \dots, n$ .

The objective is to estimate the RT distributions by focusing on the conditional distributions  $Y | R_l$ , where  $l = 1, 2$  and  $Y = \{Y_{ijk}\}_{ijk}$ . Notice that it can be extended to multiple alternatives ( $l = 1, 2, \dots, L$ ). Conditional random variables operate on a reduced sample space defined by the conditioning event. In practice, this translates to partitioning the dataset into subsets corresponding to each response outcome. Thus, we empirically split our RT data based on each response. While we model  $Y$  conditional on each response, for notational simplicity, we omit the explicit conditional notation. Therefore, we use  $Y$  instead of  $Y | R_l$ , with the understanding that we are implicitly modeling the conditional distribution.

In this experimental task, each individual’s RT result is represented as a random vector of RTs. This vector, denoted as  $Y_k = (Y_{11k}, \dots, Y_{1n_1k}, \dots, Y_{n_1k}, \dots, Y_{nn_nk})^\top$  captures the RTs across different stimuli, their levels, and replications. Here,  $\top$  indicates the transpose operation.

We consider a random sample  $Y_1, \dots, Y_m$ , where each  $Y_k$  is an independent and identically distributed (IID) random element with a cumulative distribution function  $F$ . Assuming  $F$  has a probability density function (PDF)  $f$  belonging to the Exponential Family, we propose a hierarchical GLMM structure for the

mean RTs:

$$\mu_{ijk} := E(Y_{ijk}|C_k = c_k) \text{ and } h(\mu_{ijk}) = x_{ij}^\top \beta + c_k, \quad (3)$$

where  $C_k$  represents a random effect acting as a random intercept for each individual;  $h$  denotes the ‘‘link function’’,  $\beta = (\beta_1, \dots, \beta_n)^\top$  is a fixed-effect vector of unknown regression parameters, and  $x_{ij} = (x_{ij1}, \dots, x_{ijn})^\top$  is a vector containing covariate values associated with  $\beta$ . In this context, we treat stimuli or fixed effects as categorical variables. The subscript  $i$  encompasses all stimuli types and their levels. Consequently, the  $x_{ij}$  vectors can be expressed as  $x_{ij} = (\delta_{i1}, \dots, \delta_{in})^\top$  for all  $j$ . Here,  $\delta_{ii'}$  is an indicator function: it is 1 if  $i = i'$  and 0 otherwise. This structure ensures that the elements of each  $x_{ij}$  vector always sum to 1.

For the random effects, which influence the intercept in the linear predictor, we adopt a simplified approach by considering variations only at the individual level. This means each individual has a unique random intercept. While we acknowledge the potential for incorporating other random effects, such as those related to stimuli types, difficulty levels, and within-individual correlations [e.g., using  $\{C_{ijk}\}_{ijk}$  as suggested by [Baayen and Milin \(2010\)](#)], we opt for parsimony in this initial presentation. Therefore, we assume that the random effects, denoted as  $\{C_k\}_{k=1, \dots, m}$  are IID according to a random variable  $C$  with a cumulative distribution function  $G$ . We further assume  $G$  has a continuous PDF  $g$ . This simplified random-effects structure allows us to focus on the core aspects of our approach. We leave the exploration of more complex random-effects structures for future work, as discussed in Section 4.

GLMMs inherently exhibit a relationship between the mean and variance. As described in [Tsou \(2011\)](#), this relationship can be expressed as:

$$V(Y_{ijk}) = \phi E(Y_{ijk})^\lambda, \quad (4)$$

where  $\phi$  and  $\lambda$  are constants. Different values of  $\lambda$  correspond to different distributional families. For instance,  $\lambda = 3$  is associated with the IG distribution, while  $\lambda = 2$  characterizes Gamma, lognormal or Weibull distributions [[Tsou \(2011\)](#)]. Since our hierarchical structure is developed conditional on each response, we allow the parameters in Equation 4 to vary depending on the specific response. However, we maintain the same link function  $h$  across all responses, assuming that the conditional distributions  $Y|R_l$  belong to the same family.

As discussed in Section 1, the conditional distribution of  $Y_{ijk}$  given a specific response can be theoretically modeled as the first-hitting time distribution of a diffusion process, as represented in Equation (1). The specific form of the diffusion process, also detailed in Section 1, determines the appropriate link function  $h$  for the GLMM. For example, if the diffusion process leads to an IG distribution for the RT, common link functions are  $h(\mu_{ijk}) = \log(\mu_{ijk})$  and  $h(\mu_{ijk}) = \mu_{ijk}^{-2}$ , and if the diffusion process results in a Gamma distribution for the RT, typical link functions are  $h(\mu_{ijk}) = \log(\mu_{ijk})$  and  $h(\mu_{ijk}) = \mu_{ijk}^{-1}$  [see [Dunn et al. \(2018\)](#), Chapter 11]. A key contribution of this work is establishing the connection between the parameters of the underlying cognitive process’s

diffusion, the covariates, and the fixed and random effects within the GLMM framework. This connection enables us to estimate the parameters of a diffusion process like Equation (1) for the underlying cognitive process associated with a given response by estimating the GLMM parameters.

To estimate the probability of choosing each response, we can utilize a frequency-based approach. Let  $\mathcal{I}$  represent the set of all subscripts  $(ijk)$ . For each response  $R_l$ , where  $l = 1, 2, \dots, L$ , we define  $\mathcal{I}_{R_l}$  as the subset of  $\mathcal{I}$  containing all trials with response  $R_l$ . The set of all responses in the experiment can then be expressed as the following disjoint union:

$$\mathcal{I} = \bigcup_{l=1}^L \mathcal{I}_{R_l},$$

For the RTs  $Y = \{Y_k\}_{k=1}^m$ , we define  $\Omega_{R_l} = \{Y_{ijk} : (ijk) \in \mathcal{I}_{R_l}\}$  as the set of  $Y|R_l$  results. Applying the Law of Large Numbers and Slutsky's theorem, we obtain:

$$\lim_{m \rightarrow \infty} \frac{1}{m} \sum_{i=1}^n \sum_{j=1}^{n_i} \sum_{k=1}^m \frac{\text{card}(\Omega_{R_l}^{(i,j,k)})}{n_i} = \sum_{i=1}^n \sum_{j=1}^{n_i} \frac{P(R_l^{(ij)})}{n_i}, \quad (5)$$

where convergence is in probability, and  $R_l^{(ij)}$  denotes the event of responding  $R_l$  in the  $j$ -th trial under the  $i$ -th stimulus level. Since we only consider individual-level random effects and maintain the same fixed effects for all  $j$ , the probability  $P(R_l^{(ij)})$  effectively depends only on  $i$ . Consequently, Equation (5) simplifies to  $\sum_{i=1}^n P(R_l^{(i)})$ . Alternatively, and in a more structured modeling, we could employ regression models for the responses themselves, as explored in various studies [e.g., [Van der Linden \(2007\)](#); [Moscatelli et al. \(2012\)](#); [Molenaar et al. \(2015\)](#); [Ranger et al. \(2020\)](#)]. Although in this work the main focus will not be on the modeling of the responses themselves, in Section 4 will provide a further discussion on such potential approaches.

It is important to note that Equation (5) relies on a large number of individuals in the experimental design for its validity. This requirement is often overlooked in practice. For instance, “Experiment 1” in [Suarez et al. \(2015\)](#) involved only 18 participants ( $m = 18$ ), each completing two sessions (“blocks”) of 96 trials. Participants were divided into two groups: in the “red left condition” 50% of participants responded to the color red with their left hand and green with their right, irrespective of the stimulus position on the screen; and in the “red right condition” the remaining 50% responded to red with their right hand and green with their left. Stimuli were classified as “congruent” if the stimulus and assigned hand were on the same side, and “incongruent” otherwise. This resulted in four stimuli (“green left”, “red left”, “green right”, “red right”) and two conditions (“red left”, “red right”). Combining stimuli and conditions yielded eight possible combinations ( $n = 8$ ) each representing a different level ( $i = 1, \dots, 8$ ). Trials were indexed by  $j = 1, \dots, n_i$ , with  $\sum_{i=1}^8 n_i = 2 \times 96$ . Due to the small sample size in this experiment, the consistency result in Equation (5) is not applicable.

It is worth mentioning that incorporating multiple alternative responses can introduce additional temporal and error factors. These factors arise from the time required for an individual to decide how to express their desired response (e.g., which button to press). Our model does not explicitly account for these factors, highlighting an advantage of binary choice tasks over multiple-choice (MC) tasks. Additionally, we do not consider potential fatigue effects that may arise in longer testing sessions.

Parameter estimation methods for GLMMs are well-established and extensively documented in the literature [see, e.g., [Molenberghs et al. \(2002\)](#), [Tuerlinckx et al. \(2006\)](#), [Stroup \(2012\)](#), [Lee et al. \(2018\)](#)]. These methods are readily available in popular statistical software packages like R [see also [Rönnegård et al. \(2010\)](#), [Wang et al. \(2022\)](#)]. Once we have estimated a GLMM using real data (ideally achieving good fits with a large dataset), we can investigate several aspects relevant to the experimenter: (i) stimuli and response differences aiming to analyze significant differences in RTs across various stimuli, levels, and response alternatives; (ii) response frequencies aiming to examine the frequency of different response alternatives, or the frequency of correct responses, in relation to different stimuli and their levels; and (iii) cognitive processing characteristics aiming to explore the underlying cognitive processing by establishing a theoretical link between the parameters of a mathematical model for cognitive processing and the parameters/covariates obtained from the GLMM applied to RTs conditioned on each response alternative. As mentioned above, we will focus mainly on aspects (i) and (iii), since the modeling of the responses themselves can be done using different approaches (see Section 4). We will illustrate (iii) with simple numerical examples.

Let's consider the diffusion process in Equation (1) with the following specifications:  $\{e_t\}_{t \in \mathbb{R}_+}$  is a standard Brownian,  $\theta = 0$ , and a fixed initial condition  $X_0 = a > 0$ . Under these conditions, the first-hitting time of  $X_t$  to 0 follows an IG distribution with mean  $a/\nu$  and variance  $a/\nu^3$ . For each alternative response, we can estimate the corresponding cognitive process for trial  $j$  under stimulus level  $i$  by estimating:

$$\mu_{ij} = \int E(Y_{ijk}|c)g(c)dc = E(Y_{ijk}), \quad (6)$$

where  $i = 1, \dots, n$ ,  $j = 1, \dots, n_i$ ,  $k = 1, \dots, m$ . This leads to the estimator  $\hat{\mu}_{ij} = \hat{a}_{ij}/\hat{\nu}_{ij}$ , where  $\hat{\mu}_{ij}$  is the estimate of  $\mu_{ij}$ ,  $\hat{a}_{ij}$  is the estimate of the starting processing point, and  $\hat{\nu}_{ij}$  is the estimate of the mean rate of information accumulation. Furthermore, by estimating the variance:

$$\sigma_{ij}^2 = \int V(Y_{ijk}|c)g(c)dc + \int E(Y_{ijk}|c)^2g(c)dc - \mu_{ij}^2 = V(Y_{ijk}), \quad (7)$$

where  $i = 1, \dots, n$ ,  $j = 1, \dots, n_i$ ,  $k = 1, \dots, m$ , we obtain the estimator  $\hat{\sigma}_{ij}^2 = \hat{a}_{ij}/\hat{\nu}_{ij}^3$ . This allows us to derive  $\sqrt{\hat{\mu}_{ij}/\hat{\sigma}_{ij}^2} = \hat{\nu}_{ij}$  and  $\hat{\mu}_{ij}\hat{\nu}_{ij} = \hat{a}_{ij}$ . Therefore, we can estimate the underlying cognitive process described by Equation (1) by estimating the parameters of our GLMM for each alternative response. This

estimation provides a distributional representation of the cognitive mechanism leading to the observed response.

*Remark.* Since we are solely considering individual-level random effects and maintaining consistent fixed effects across all trials  $j$ , Equations (6) and (7) effectively become independent of  $j$ . However, this can be extended by incorporating random effects within individuals, as discussed in Section 4.

To demonstrate this concept in a simplified scenario, we simulate independent and identically distributed (IID) responses, denoted as  $\{Y_u\}_u$ , where  $E(Y_u) = \mu$  and  $V(Y_u) = \mu^3$ . This implies that the responses follow an IG distribution, as obtained by setting  $\lambda = 3$  and  $\phi = 1$  in Equation (4),  $V(Y_u) = \phi E(Y_u)^\lambda$ . We generate four datasets, each containing 1000 observations, with  $\mu = 2$ ,  $\mu = 1.5$ ,  $\mu = 1$  and  $\mu = 0.5$ , respectively. For each dataset, we estimate the corresponding values of  $\mu$  and  $\phi$ . Subsequently, we simulate the respective RTs based on Equations (1)-(2) using the following scheme:

1. Fix  $X_0 = \sqrt{1/\hat{\phi}}$  and  $\delta = 0.01$ .
2. Iterate recursively

$$X_{(t)} = X_{(t-1)} - \frac{1}{\hat{\mu}} \sqrt{\frac{1}{\hat{\phi}}} \delta + \sqrt{\delta} \epsilon_{(t)},$$

with  $t = 1, 2, \dots$ , and where the  $\epsilon_{(t)}$ 's are IID standard normal distributed.

3. The above process continues until the first  $t = t^*$  such that  $X_{(t^*)} \leq 0$ .
4. The simulated RT is given by  $T^* = t^* \delta$ .
5. We replicate this  $M$  times, obtaining a random sample of RTs  $T_1^*, T_2^*, \dots, T_M^*$ .
6. Finally, we assess the goodness-of-fit of these simulated RT datasets against the theoretical IG distributions they were originally generated from (those with  $\mu = 2$ ,  $\mu = 1.5$ ,  $\mu = 1$  and  $\mu = 0.5$ , and with  $\phi = 1$  in each case). The results of this goodness-of-fit evaluation are presented in Figure 1.

We can establish a similar algorithm to simulate RTs with a Gamma distribution and reconstruct the underlying cognitive process represented by Equation (1). This approach, employed in [Tejo et al. \(2019\)](#) and based on the findings of [Jackson et al. \(2009\)](#), proceeds as follows: (i) generate IID responses, denoted as  $\{Y_u\}_u$ , with  $E(Y_u) = \mu = \alpha\beta$  and  $V(Y_u) = (1/\alpha)\mu^2 = \alpha\beta^2$ . This corresponds to setting  $\lambda = 2$  and  $\phi = 1/\alpha$  in Equation (4),  $V(Y_u) = \phi E(Y_u)^\lambda$ , resulting in Gamma-distributed responses with shape parameter  $\alpha$  and scale parameter  $\beta$ ; (ii) estimate the values of  $\alpha$  and  $\beta$  from the generated datasets; and (iii) simulate the corresponding RTs based on Equations (1)-(2) using the following scheme:

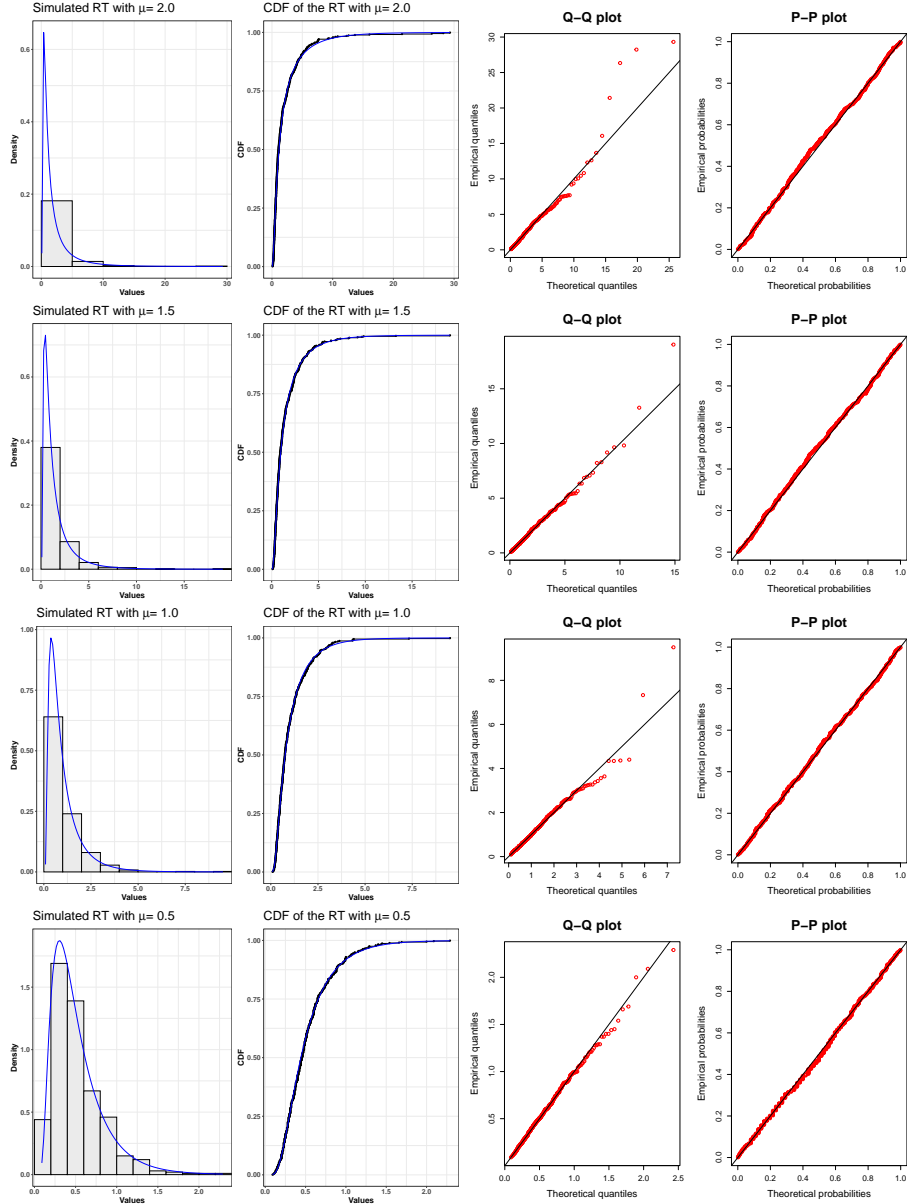


Figure 1: Plots displaying the goodness-of-fit assessment for simulated IG data. Each row corresponds to a different simulated dataset with a specific mean ( $\mu = 2, \mu = 1, 5, \mu = 1$  and  $\mu = 0.5$ , from top to bottom). In all cases, the scale parameter ( $\phi$ ) was set to 1. From left to right, each row shows the estimated PDF via a histogram of the simulated data with the theoretical IG PDF overlaid in blue; estimated CDF showing the empirical CDF of the simulated data with the theoretical IG CDF overlaid in blue; Quantile-Quantile (Q-Q) Plot comparing the quantiles of the simulated data to the quantiles of the theoretical IG distribution; and Probability-Probability (P-P) Plot comparing the cumulative probabilities of the simulated data to the cumulative probabilities of the theoretical IG distribution. For each case, 1000 random variables  $Y_1, \dots, Y_{1000}$  were simulated, and the recursive scheme was replicated 500 times to obtain the corresponding RTs ( $T_1^*, \dots, T_{500}^*$ ).

1. Fix some  $\delta$  small, and consider  $\theta = 0$ . The initial value  $X_0$  is taken from the sum of two independent Gamma with common shape and scale  $\hat{\alpha}$  and  $\sqrt{\hat{\beta}/2}$ , respectively.
2. Iterate recursively

$$X_{(t)} = X_{(t-1)} - \sqrt{\hat{\beta}/2}^{-1} \delta + \sqrt{\delta} \epsilon_{(t)},$$

with  $t = 1, 2, \dots$ , and where the  $\epsilon_{(t)}$ 's are IID standard normal distributed.

3. The above process continues until the first  $t = t^*$  such that  $X_{(t^*)} \leq 0$ .
4. The simulated RT is given by  $T^* = t^* \delta$ .
5. We replicate this  $M$  times (independently), obtaining a random sample of RTs  $T_1^*, T_2^*, \dots, T_M^*$ .
6. We finally verify the goodness-of-fit of such RT sets with respect to the theoretical distribution for each data set originally simulated (See Fig. 2).

*Remark.* Theoretical models, while simple, can enable estimations of parameter  $\theta$  in equation (1) with relative ease [Tejo et al. (2019)]. However, the hierarchical nature of our model, described in Equation (3), presents a challenge when incorporating a parameter for subsequently estimating  $\theta$ . Consequently, our reconstruction will adhere to a scheme resembling equation (1) but with  $\theta$  set to 0. The integration of this parameter into the GLMM is reserved for future consideration.

The following section details the application of our methodology to “Experiment 1” documented in Marmolejo-Ramos et al. (2020).

### 3 Experiment and statistical data analysis

*Description of the experiment and database.* Participants were instructed to identify a facial expression as “sad” or “happy” as quickly and accurately as possible, either while holding a pen in their teeth or with no pen. Across seven blocks, each containing all 11 stimuli, the 11 faces were presented twice in a randomized order. Consequently, each stimulus was displayed 77 times under each of the two conditions (pen-in-teeth and no-pen), resulting in a total of 154 trials [for a comprehensive description of the experiment, see Marmolejo-Ramos et al. (2020)].

The 11 stimuli ranged from a “fully sad” facial expression (designated as “stimulus 0”) to a “fully happy” one (designated as “stimulus 10”). Given the two experimental conditions (pen-in-teeth and no-pen), we treated the combined levels of all stimulus types as a set of 22 unique levels. These levels were indexed as follows:  $i = 1$  representing “stimulus 0 + pen-in-teeth”,  $i=2$  representing

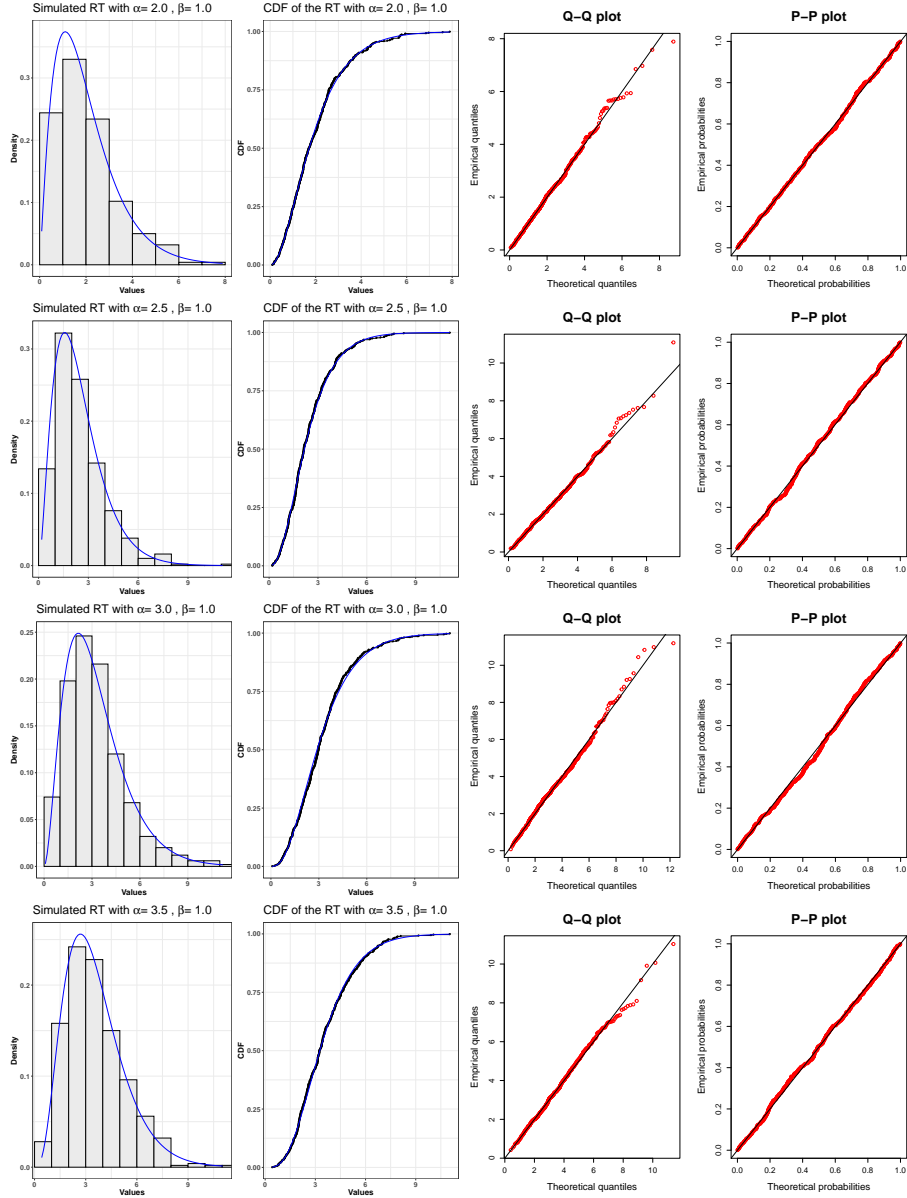


Figure 2: Plots displaying the goodness-of-fit assessment for simulated Gamma data. Each row corresponds to a different shape parameter value ( $\alpha = 2$ ,  $\alpha = 2.5$ ,  $\alpha = 3$  and  $\alpha = 3.5$ , from top to bottom). In all cases, the scale parameter ( $\beta$ ) was set to 1. From left to right, each row shows the estimated PDF via a histogram of the simulated data with the theoretical Gamma PDF overlaid in blue; estimated CDF showing the empirical CDF of the simulated data with the theoretical Gamma CDF overlaid in blue; Quantile-Quantile (Q-Q) Plot comparing the quantiles of the simulated data to the quantiles of the theoretical Gamma distribution; and Probability-Probability (P-P) Plot comparing the cumulative probabilities of the simulated data to the cumulative probabilities of the theoretical Gamma distribution. For each case, 1000 random variables  $Y_1, \dots, Y_{1000}$  were simulated, and the recursive scheme was replicated 500 times with  $\delta = 0.01$  to obtain the corresponding RTs ( $T_1^*, \dots, T_{500}^*$ ).

“stimulus 1 + pen-in-teeth”, and so on, up to  $i = 11$  for “stimulus 10 + pen-in-teeth”. The indexing continued with  $i = 12$  for “stimulus 0 + no-pen” and concluded with  $i = 22$  for “stimulus 10 + no-pen”.

The study involved 116 participants ( $k = 1, \dots, 116$ ), each exposed to every combined stimulus level seven times across seven “blocks”; thus,  $j = 1, \dots, 7$  represents the block number. Participants provided binary responses, categorized as  $R_1$ : “sad” or  $R_2$ : “happy”.

The fixed-effects parameter vector  $\beta$  in Equation (3) consists of 22 components:  $\beta = (\beta_1, \dots, \beta_{22})^\top$ . For the random effects, we considered 116 IID Normal variables  $\{C_k\}_{k=1, \dots, 116}$  with mean 0 and variance  $\tau^2$ . Both IG and Gamma models employed the logarithmic link function. The parameters were estimated using Maximum Likelihood (ML) methods, implemented using the *glmer* function from the *lme4* package in **R**. This function computes ML estimates for GLMMs by approximating the log-likelihood through Gauss-Hermite quadrature and maximizing it via numerical optimization. The complete code and dataset are available at <https://cutt.ly/feXh490H>. The parameter estimates for the Gamma model are displayed in Fig. 3.

Due to convergence issues in the iterative numerical method used to calculate estimation errors, we were unable to obtain all the confidence intervals for the IG model (this will be discussed in detail in Section 4). Figure 4 therefore presents only those fixed-effects estimates for which we successfully computed the estimation errors.

Our analysis reveals a consistent pattern in RTs across both emotional classifications. As shown in Figs. 3 and 4, the left plots demonstrate that participants who correctly identified unambiguous “sad” faces (stimulus 0 and 1) exhibited faster RTs with minimal variance. In contrast, when participants misclassified clearly “happy” faces (stimulus 9 and 10) as “sad”, their RTs were notably slower with increased variability, though this pattern was observed in only a small subset of participants. The right plots in Figs. 3 and 4 present a symmetrical pattern: correct classification of unambiguous “happy” faces (stimulus 9 and 10) resulted in faster RTs with low variability, while misclassification of clearly “sad” faces (stimulus 0 and 1) as “happy” led to slower RTs with higher variability, again observed in a limited number of participants.

The Akaike Information Criterion (AIC) values were as follows: 126498.837 and 126122.440 for the Gamma model under “sad” and “happy” responses, respectively, and 149001.247 and 149739.235 for the IG model under “sad” and “happy” responses, respectively. These results suggest that while the IG model exhibits lower variability in terms of error and random effects, the Gamma model demonstrates a superior fit based on likelihood.

Given that the link function is log and the  $C_k$ ’s are IID as normal with a mean of 0 and variance  $\tau^2$ , we can derive the  $\mu_i$ ’s using Equation (6) in our specific application:

$$\mu_i = \int \exp(x_{ij}^\top \beta + c) \phi_{0, \tau^2}(c) dc = \int \exp(\beta_i + c) \phi_{0, \tau^2}(c) dc$$

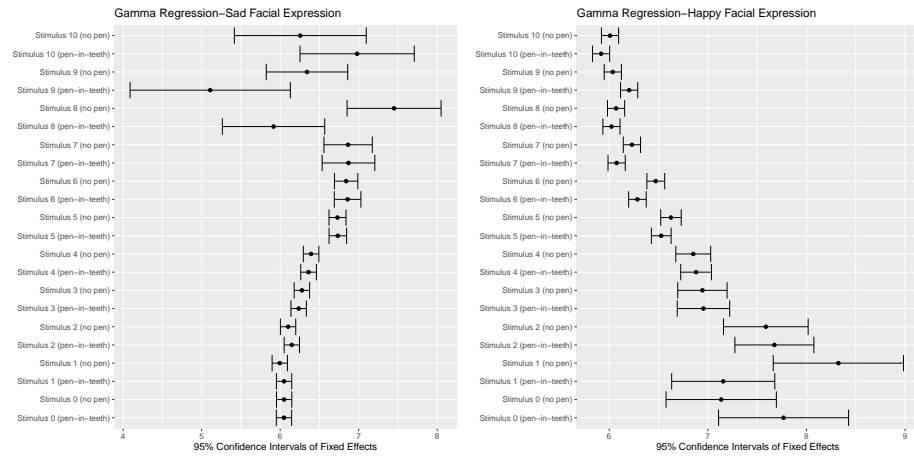


Figure 3: Fixed-effects estimation results under the Gamma model, displaying point estimates (dots) and their associated 95% confidence intervals for all stimulus combinations. The figure is divided into two panels: the left panel presents results for “sad” facial expression responses, while the right panel shows results for “happy” facial expression responses. For “sad” responses, the estimated random-effect variance per individual ( $\hat{\tau}^2$ ) was approximately 0.18, with an error variance of approximately 0.62. For “happy” responses, the random-effect variance was approximately 0.13, with an error variance of approximately 0.61.

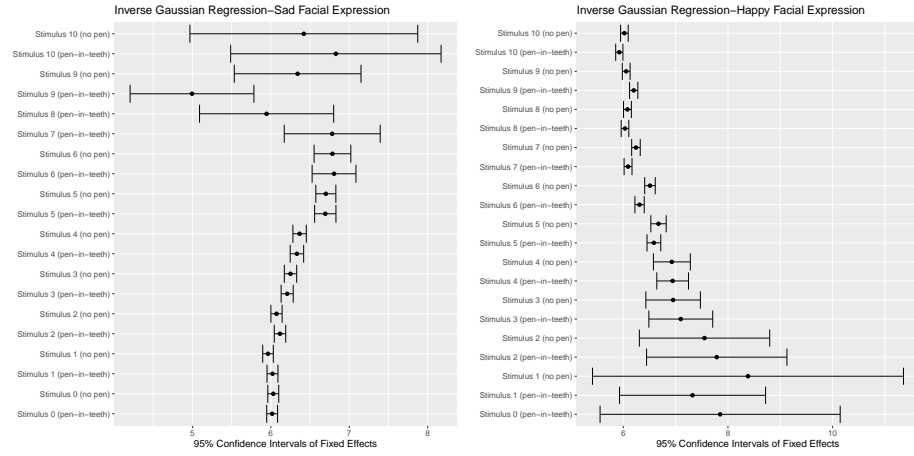


Figure 4: Fixed-effects estimation results under the IG model, displaying point estimates (dots) and their associated 95% confidence intervals for most stimulus combinations. The figure is divided into two panels: the left panel presents results for “sad” facial expression responses, while the right panel shows results for “happy” facial expression responses. For “sad” responses, the estimated random-effect variance per individual ( $\hat{\tau}^2$ ) was approximately 0.01, with an error variance of approximately 0.05. For “happy” responses, the random-effect variance was approximately 0.00, also with an error variance of approximately 0.05. Note that confidence intervals could not be obtained for all stimulus combinations due to numerical convergence issues.

$$= \exp\left(\beta_i + \frac{\tau^2}{2}\right),$$

where  $\phi_{0,\tau^2}(\cdot)$  is the probability density of a  $N(0, \tau^2)$ . Then, we can estimate the (marginal) expectation of the  $Y_{ijk}$ 's as:

$$\hat{\mu}_i = \exp\left(\hat{\beta}_i + \frac{\hat{\tau}^2}{2}\right).$$

For the marginal variance expressed in Equation (7), we can derive its components as follows: The first term,  $\int E(Y_{ijk}|c)^2 \phi_{0,\tau^2}(c) dc$  equals  $\exp(2\beta_i + 2\tau^2)$ , while  $\mu_i^2$  is equal to  $\exp(2\beta_i + \tau^2)$ . Furthermore, the integral  $\int V(Y_{ijk}|c) \phi_{0,\tau^2}(c) dc$  represents the error variance, which we will denote by  $\sigma^2$ . Therefore, we can express  $\sigma_i^2$  as:

$$\begin{aligned}\sigma_i^2 &= \sigma^2 + \exp(2\beta_i + 2\tau^2) - \exp(2\beta_i + \tau^2) \\ &= \sigma^2 + \exp(2\beta_i + 2\tau^2) (1 - \exp(-\tau^2)).\end{aligned}$$

So, an estimator of  $\hat{\sigma}_i^2$  is:

$$\hat{\sigma}_i^2 = \hat{\sigma}^2 + \exp(2\hat{\beta}_i + 2\hat{\tau}^2) (1 - \exp(-\hat{\tau}^2)),$$

where  $\hat{\sigma}^2$  is the estimated error variance.

With these components established, we can now reconstruct the underlying cognitive processes for each stimulus combination and response type, following the methodology outlined in Section 2.

*Remark.* The explicit derivation of expressions (6)-(7) was made possible by our specific model choices: the logarithmic link function  $h(\cdot) = \log(\cdot)$  and normally distributed random-effects. For alternative specifications of these components, these expressions may not have analytical solutions and would require numerical approximation methods.

## 4 Discussion and scopes

This paper demonstrates a relatively straightforward method for connecting two methodological approaches to modeling RTs. The first approach models RTs as the result of the distribution of the first-hitting time of a simple diffusion process, simulating the cognitive processing underlying the choice of a response in a choice task. The second approach utilizes a (conditional) GLMM framework. The advantage of this connection is twofold. First, starting with the diffusion model approach, theoretical models can be used to inform the selection of specific GLMM families. Second, after estimating the parameters within these GLMM families, conditioned on each response, we can “reconstruct” a simplified model of the underlying cognitive process that generated those responses.

While the presented approach involves certain simplifications, it offers potential for extension and generalization. For instance, within the GLMM framework, we could incorporate additional random effects to account for correlations within individual responses, and explore alternative link functions and transformations, as discussed in [Lo and Andrews \(2015\)](#). Furthermore, the initial diffusion model describing the cognitive process behind a specific response included a “non-decision” parameter, which was ultimately set to zero here for simplicity. Investigating the estimation of this parameter through a revised GLMM formulation could be a valuable avenue for future research.

It is important to note that our primary focus was on modeling RTs conditional on the responses, rather than on the responses themselves. While a simplified approach to modeling response probabilities is presented in Equation (5), a more rigorous treatment is warranted. This is because responses are also influenced by fixed effects at different stimulus levels and by random effects associated with individuals, as highlighted in previous research [[Van der Linden \(2007\)](#); [Moscatelli et al. \(2012\)](#); [Molenaar et al. \(2015\)](#); [Ranger et al. \(2020\)](#)].

Estimating GLMMs via ML typically requires numerical quadrature methods, as a closed-form analytical solution is unavailable. Popular choices include the Laplace approximation and adaptive Gauss-Hermite quadrature. However, these methods have been shown to produce biased estimators in certain contexts [[Rabe-Hesketh et al. \(2005\)](#)], and alternative approaches may be superior for GLMMs [[Handayani et al. \(2017\)](#)]. Stochastic Expectation-Maximization (EM) algorithms, such as the Stochastic Approximation EM (SAEM) algorithm [[Delyon et al. \(1999\)](#)], offer an alternative to log-likelihood approximation methods. The SAEM algorithm has shown promising performance with complex mixed models like GLMMs, while retaining the advantages of the EM framework [[Savic and Lavielle \(2009\)](#); [Meza et al. \(2009\)](#)]. Therefore, a worthwhile future direction would be to explore the application of the SAEM algorithm for estimating the model presented in this work.

We believe that our approach can be extended to other variants of GLMs, particularly the Double Hierarchical GLM (DHGLM). Despite its significant potential, the DHGLM, a sophisticated extension of GLMs, has not yet been applied to RT experiments. Its primary innovation is the inclusion of random effects in both the mean and dispersion components of the model. This dual inclusion allows for the simultaneous modeling of heteroscedasticity between clusters and heterogeneity in means, offering a more comprehensive analytical framework. A key advantage of the DHGLM is its use of  $h$ -likelihood, which provides a unified framework for model fitting through a single algorithm, thus avoiding the need for complex numerical integration or specifications of prior probabilities, leading to computational efficiency and practical implementation [[Lee and Nelder \(2006\)](#)]. We propose that our conditional GLMM approach could be integrated into the DHGLM framework, leveraging the mean and shape parameters of the IG distribution and the shape and scale parameters of the Gamma distribution. This integration would facilitate more advanced analyses of RT responses, potentially yielding deeper insights into the underlying cognitive processes.

Considering the points discussed above and the demonstrated applicability shown in previous sections, the presented approach provides a solid foundation for further extensions. These extensions hold the potential to enhance the analysis and interpretation of experimental results, and broaden the applicability of the approach to multiple-choice task tests.

### **Data availability statement**

All data are available on link <https://cutt.ly/feXh490H>.

### **Acknowledgements**

This research was funded by the INICI-UV Grant (UVA 20993, 2021) and received additional support from Exploration-ANID (13220168, 2022). The authors extend their gratitude to Professor Javier Contreras, Professor Joaquín Cavieres, and Professor Raydonal Ospina for their invaluable insights and assistance with numerical implementations.

### **Disclosure Statement**

The authors declare that they have no conflicts of interest of any kind.

## **References**

Anders, R., Alario, F., Van Maanen, L., et al. (2016). The shifted wald distribution for response time data analysis. *Psychological methods*, 21(3), 309.

Baayen, R. H., & Milin, P. (2010). Analyzing reaction times. *International Journal of Psychological Research*, 3(2), 12–28.

Balakrishnan, N., Leiva, V., Sanhueza, A., & Cabrera, E. (2009). Mixture inverse gaussian distributions and its transformations, moments and applications. *Statistics*, 43(1), 91–104.

Balota, D. A., & Yap, M. J. (2011). Moving beyond the mean in studies of mental chronometry: The power of response time distributional analyses. *Current Directions in Psychological Science*, 20(3), 160–166.

Blurton, S. P., Kesselmeier, M., & Gondan, M. (2017). The first-passage time distribution for the diffusion model with variable drift. *Journal of Mathematical Psychology*, 76, 7–12.

Brown, S. D., & Heathcote, A. (2008). The simplest complete model of choice response time: Linear ballistic accumulation. *Cognitive psychology*, 57(3), 153–178.

De Boeck, P., & Jeon, M. (2019). An overview of models for response times and processes in cognitive tests. *Frontiers in psychology*, 10, 102.

Delyon, B., Lavielle, M., & Moulines, E. (1999). Convergence of a stochastic approximation version of the EM algorithm. *Annals of Statistics*, 94–128.

Desmond, A. F. (1986). On the relationship between two fatigue-life models. *IEEE Transactions on Reliability*, 35(2), 167–169.

Donkin, C., & Brown, S. D. (2018). Response times and decision-making. *Stevens' handbook of experimental psychology and cognitive neuroscience*, 5, 1–33.

Dunn, P. K., Smyth, G. K., et al. (2018). *Generalized linear models with examples in r* (Vol. 53). Springer.

Handayani, D., Notodiputro, K. A., Sadik, K., & Kurnia, A. (2017, 03). A comparative study of approximation methods for maximum likelihood estimation in generalized linear mixed models (GLMM). *AIP Conference Proceedings*, 1827(1), 020033. doi: 10.1063/1.4979449

Horrocks, J., & Thompson, M. E. (2004). Modeling event times with multiple outcomes using the wiener process with drift. *Lifetime Data Analysis*, 10(1), 29–49.

Jackson, K., Kreinin, A., & Zhang, W. (2009). Randomization in the first hitting time problem. *Statistics & probability letters*, 79(23), 2422–2428.

LaBerge, D. (1962). A recruitment theory of simple behavior. *Psychometrika*, 27(4), 375–396.

Lee, Y., & Nelder, J. A. (2006). Double hierarchical generalized linear models. *Journal of the Royal Statistical Society: Series C (Applied Statistics)*, 55(2), 139–185. doi: 10.1111/j.1467-9876.2006.00538.x

Lee, Y., Nelder, J. A., & Pawitan, Y. (2018). *Generalized linear models with random effects: unified analysis via h-likelihood*. Chapman and Hall/CRC.

Leiva, V., Tejo, M., Guiraud, P., Schmachtenberg, O., Orio, P., & Marmolejo-Ramos, F. (2015). Modeling neural activity with cumulative damage distributions. *Biological Cybernetics*, 109(4), 421–433.

Lo, S., & Andrews, S. (2015). To transform or not to transform: Using generalized linear mixed models to analyse reaction time data. *Frontiers in psychology*, 6, 1171.

Marmolejo-Ramos, F., Cousineau, D., Benites, L., & Maehara, R. (2015). On the efficacy of procedures to normalize ex-gaussian distributions. *Frontiers in psychology*, 5, 1548.

Marmolejo-Ramos, F., & González-Burgos, J. (2013). A power comparison of various tests of univariate normality on ex-gaussian distributions. *Methodology*.

Marmolejo-Ramos, F., Murata, A., Sasaki, K., Yamada, Y., Ikeda, A., Hinojosa, J. A., ... Ospina, R. (2020). Your face and moves seem happier when i smile. *Experimental psychology*.

Marmolejo-Ramos, F., Vélez, J. I., & Romão, X. (2015). Automatic detection of discordant outliers via the ueda's method. *Journal of Statistical Distributions and Applications*, 2(1), 1–14.

Matzke, D., & Wagenmakers, E.-J. (2009). Psychological interpretation of the ex-gaussian and shifted wald parameters: A diffusion model analysis. *Psychonomic bulletin & review*, 16(5), 798–817.

McCulloch, C. E., & Neuhaus, J. M. (2005). Generalized linear mixed models. *Encyclopedia of biostatistics*, 4.

Meyer, D. E., Osman, A. M., Irwin, D. E., & Yantis, S. (1988). Modern mental chronometry. *Biological psychology*, 26(1-3), 3–67.

Meza, C., Jaffrézic, F., & Foulley, J.-L. (2009). Estimation in the probit normal model for binary outcomes using the saem algorithm. *Computational Statistics & Data Analysis*, 1350-1360.

Molenaar, D., Tuerlinckx, F., & van der Maas, H. L. (2015). A bivariate generalized linear item response theory modeling framework to the analysis of responses and response times. *Multivariate Behavioral Research*, 50(1), 56–74.

Molenberghs, G., Renard, D., & Verbeke, G. (2002). A review of generalized linear mixed models. *Journal de la Société Française de Statistique*, 143(1-2), 53–78.

Moscatelli, A., Mezzetti, M., & Lacquaniti, F. (2012). Modeling psychophysical data at the population-level: The generalized linear mixed model. *Journal of Vision*, 12(11), 26–26.

Osmon, D. C., Kazakov, D., Santos, O., & Kassel, M. T. (2018). Non-gaussian distributional analyses of reaction times (rt): improvements that increase efficacy of rt tasks for describing cognitive processes. *Neuropsychology Review*, 28(3), 359–376.

Palmer, E. M., Horowitz, T. S., Torralba, A., & Wolfe, J. M. (2011). What are the shapes of response time distributions in visual search? *Journal of Experimental Psychology: Human Perception and Performance*, 37(1), 58.

Posner, M. I. (2005). Timing the brain: Mental chronometry as a tool in neuroscience. *PLoS Biology*, 3(2), e51.

Rabe-Hesketh, S., Skrondal, A., & Pickles, A. (2005). Maximum likelihood estimation of limited and discrete dependent variable models with nested random effects. *Journal of Econometrics*, 128(2), 301-323. doi: <https://doi.org/10.1016/j.jeconom.2004.08.017>

Ranger, J., Kuhn, J.-T., & Gaviria, J.-L. (2015). A race model for responses and response times in tests. *Psychometrika*, 80(3), 791–810.

Ranger, J., Kuhn, J. T., & Ortner, T. M. (2020). Modeling responses and response times in tests with the hierarchical model and the three-parameter lognormal distribution. *Educational and Psychological Measurement*, 80(6), 1059–1089.

Ratcliff, R. (1978). A theory of memory retrieval. *Psychological Review*, 85(2), 59.

Ratcliff, R., & Tuerlinckx, F. (2002). Estimating parameters of the diffusion model: Approaches to dealing with contaminant reaction times and parameter variability. *Psychonomic Bulletin & Review*, 9(3), 438–481.

Ratcliff, R., & Van Dongen, H. P. (2011). Diffusion model for one-choice reaction-time tasks and the cognitive effects of sleep deprivation. *Proceedings of the National Academy of Sciences*, 108(27), 11285–11290.

Rohrer, D., & Wixted, J. T. (1994). An analysis of latency and interresponse time in free recall. *Memory & Cognition*, 22(5), 511–524.

Rönnegård, L., Shen, X., & Alam, M. (2010). hglm: A package for fitting hierarchical generalized linear models. *The R Journal*, 2(2), 20–28.

Rousselet, G. A., & Wilcox, R. R. (2020). Reaction times and other skewed distributions: problems with the mean and the median. *Meta-Psychology*, 4.

Savic, R., & Lavielle, M. (2009). Performance in population models for count data, part II: a new SAEM algorithm. *Journal of Pharmacokinetics and Pharmacodynamics*, 36, 367–379.

Smith, E. E. (1968). Choice reaction time: An analysis of the major theoretical positions. *Psychological Bulletin*, 69(2), 77.

Stroup, W. W. (2012). *Generalized linear mixed models: modern concepts, methods and applications*. CRC press.

Suarez, I., Vidal, F., Burle, B., & Casini, L. (2015). A dual-task paradigm to study the interference reduction in the simon task. *Experimental Psychology*.

Tejo, M., Araya, H., Niklitschek-Soto, S., & Marmolejo-Ramos, F. (2019). Theoretical models of reaction times arising from simple-choice tasks. *Cognitive Neurodynamics*, 13(4), 409–416.

Tejo, M., Niklitschek-Soto, S., & Marmolejo-Ramos, F. (2018). Fatigue-life distributions for reaction time data. *Cognitive Neurodynamics*, 12(3), 351–356.

Tsou, T.-S. (2011). Determining the mean–variance relationship in generalized linear models—a parametric robust way. *Journal of Statistical Planning and Inference*, 141(1), 197–203.

Tuerlinckx, F., Rijmen, F., Verbeke, G., & De Boeck, P. (2006). Statistical inference in generalized linear mixed models: A review. *British Journal of Mathematical and Statistical Psychology*, 59(2), 225–255.

Usher, M., Olami, Z., & McClelland, J. L. (2002). Hick’s law in a stochastic race model with speed–accuracy tradeoff. *Journal of Mathematical Psychology*, 46(6), 704–715.

Van der Linden, W. J. (2007). A hierarchical framework for modeling speed and accuracy on test items. *Psychometrika*, 72(3), 287–308.

Vélez, J. I., Correa, J. C., & Marmolejo-Ramos, F. (2015). A new approach to the box–cox transformation. *Frontiers in Applied Mathematics and Statistics*, 1, 12.

Villegas, C., Paula, G. A., & Leiva, V. (2011). Birnbaum-saunders mixed models for censored reliability data analysis. *IEEE Transactions on Reliability*, 60(4), 748–758.

Wainer, H. (1977). Speed vs reaction time as a measure of cognitive performance. *Memory & Cognition*, 5(2), 278–280.

Wang, T., Graves, B., Rosseel, Y., & Merkle, E. C. (2022). Computation and application of generalized linear mixed model derivatives using lme4. *Psychometrika*, 1–21.

Woodrow, H. (1911). Reaction times. *Psychological Bulletin*, 8(11), 387.

Woods, D. L., Wyma, J. M., Yund, E. W., Herron, T. J., & Reed, B. (2015). Factors influencing the latency of simple reaction time. *Frontiers in Hu-*

*man Neuroscience*, 9, 131.